Photocyclization of Substituted Allyl Radicals and Properties of the Resulting Cyclopropyl Radicals

V. A. Radzig,[†] L. Yu. Ustynyuk,[‡] N. Yu. Osokina,[‡] V. I. Pergushov,[‡] and M. Ya. Mel'nikov*[,‡]

N. N. Semenov Institute of Chemical Physics, Moscow 117334, Russia, and Department of Chemistry, M. V. Lomonosov Moscow State University, Moscow 119899, Russia

Received: March 25, 1997; In Final Form: January 27, 1998

The photochemical transformations of the substituted allyl radicals $\equiv Si(CH_2)_mCH{=}{=}CH{=}{=}CH_2$ ($m = 0$, 1, or 3) and $\equiv SiO(CH_2)_mCH{=}{=}CH{=}{=}CH_2$ ($m = 0-3$) grafted onto a silica surface were studied. The cyclization of the allyl-type radicals resulting in the formation of the corresponding β-substituted cyclopropyl radicals $\equiv Si(CH_2)_m$-c-Pr$^\bullet$ or $\equiv SiO(CH_2)_m$-C-Pr$^\bullet$ (c-Pr = cyclopropyl) was found to be the primary photochemical process occurring upon photolysis at $\lambda \geq 370$ nm. Further transformations of the resulting cyclopropyl radicals depend crucially on the m value. In the case of $m = 0$ or 1, the thermal isomerization of the cyclopropyl-type radicals yielding the parent allyl-type radicals is the main reaction pathway at room temperature. For $m = 2$ or 3 the reaction of intramolecular hydrogen atom transfer becomes the predominating process. This reaction results in the corresponding alkyl-type radicals $\equiv SiCH(CH_2)_{m-1}$-c-Pr$^\bullet$ or $\equiv SiO\dot{C}H(CH_2)_{m-1}$-c-Pr formation. It was shown that the presence of electron-withdrawing substituents in β-position resulted in the decrease in the thermal stability of the cyclopropyl-type radicals. The experimental data obtained were compared with the results of quantum-chemical calculations.

Introduction

Allyl-type radicals occur as important intermediates in various processes involving organic compounds, such as thermal, photochemical, radiation-induced, and mechanochemical reactions. The mechanisms of their formation and reactions of these radicals were commonly studied in the solid phase, i.e., in organic glasses or polymers. Under the conditions of restricted molecular motion, the allyl-type radicals are rather stable because their reactivity in the processes of substitution and addition to multiple bonds is comparatively low.

A sharp increase in the reactivity of the allyl-type radicals is observed under the photoexcitation. According to available experimental and theoretical data,[1−4] the absorbtion of allyl radicals is due to two partially overlapping electronic transitions. The maxima of the corresponding bands are positioned at ca. 240 and 400 nm.

Allyl-type radicals in the electronically excited states undergo chemical transformations. The results of the previous studies concerning the photochemistry of allyl radicals in solid organic matrixes allow for the possibilities of both intramolecular reactions and intermolecular processes including the electronically excited states of allyl radicals and surrounding matrix molecules. Under these conditions, the elucidation of the mechanism of the primary photochemical reaction is a rather complicated problem. Several hypotheses about the mechanism of the phototransformation of allyl radicals in the systems under consideration were proposed. In particular, it was suggested[5,6] that the principal reaction of the allyl-type macroradicals in polyethylene occurring upon photolysis at $\lambda \geq 390$ was the scission of the C−C bond in β-position to the radical site. These data are in disagreement with the results obtained in the studies of the photochemical transformations of allyl radicals upon photolysis in the range 360−410 nm in various frozen matrixes at 77 K.[7−9] In the latter case, it was concluded that the excited allyl radicals abstracted hydrogen atoms from the matrix molecules.

The IR spectroscopic studies[10] revealed that the photocyclization of allyl radical to yield cyclopropyl radical occurred upon photolysis at $\lambda = 410$ nm in an argon matrix at 18 K (note that the possibility of the secondary intermolecular reactions of the electronically excited radical is excluded in this case). However, to our knowledge, the possibility of photocyclization was still neglected in the discussion of the mechanisms of the phototransformations of the allyl-type radicals in hydrocarbon matrixes.

Thus, the photoreactions of the allyl-type radicals in organic matrixes result in formation of various stable products. However, the specific scheme of the elementary reactions resulting in the formation of the products observed is still not clear. Evidence for the possibility of photocyclization was obtained only for the simplest allyl-type radical.[10] The corresponding data for the allyl-type radicals of a more complex structure are unavailable.

In this contribution we report the results of the study of the mechanisms of phototransformations of the allyl-type radicals of general structure with various m (X = ≡Si or ≡Si−O) upon photolysis at $\lambda \geq 370$ nm and subsequent thermal reactions of the radical intermediates.

As a pattern, we investigated allyl radicals grafted onto a silica surface. This technique for preparation of immobilized radicals and analysis of their thermal and photochemical reactions was developed only recently.[11,12] For this reason, we will consider briefly main specific features of the method applied.

* To whom correspondence should be addressed. Fax: 7(095)9328846. E-mail: melnikov@melnik.chem.msu.su.
[†] N. N. Semenov Institute of Chemical Physics.
[‡] M. V. Lomonosov Moscow State University.

S1089-5639(97)01065-7 CCC: $15.00
Published on Web 06/19/1998

TABLE 1: Structure and Concentration of the Surface Defects Trapped at the Silica Surface upon Using Various Activation Techniques

structure and concentration of surface defects, m^{-2}	≡Si•	≡SiO•	=Si•	=Si=O
thermochemical activation[14a]	$\approx 6 \times 10^{15}$		$\approx 9 \times 10^{16}$	
photochemical activation[15]	$\approx 10^{14}$	$\approx 7 \times 10^{14}$	$\leq 10^{13}$	$\leq 10^{13}$
mechanochemical activation[16]	$\approx 2 \times 10^{16}$	$\approx 2 \times 10^{16}$	$\approx 10^{15}$	$\approx 10^{17}$

[a] ESR spectra of the silica samples after termochemical activation show the single line with $g = 2.0026$, which may be attributed to ≡C•.

The structure of defects stabilized on the silica surface activated by various techniques was analyzed in refs 13−15. Various activation procedures result in the stabilization of the surface defects of two main types, i.e., the paramagnetic species of the structures $(\equiv Si-O-)_3Si^{\bullet}$ and $(\equiv Si-O-)_3Si-O^{\bullet}$ and the diamagnetic species of the structures $(\equiv Si-O-)_2Si^{\bullet}$ and $(\equiv Si-O-)_2Si=O$. The paramagnetic surface defects exhibit high reactivity in the reactions of addition to unsaturated compounds,[11,12] which makes it possible to produce various radical groups grafted onto the silica surface. The resulting intermediates are chemically attached to the surface and sterically available for the attack of the surrounding molecules. The direct environment of the intermediates consists of chemically inert siloxane bonds. Using this technique makes it possible to prepare various kinds of intermediates and to study their spectral characteristics by ESR, IR, UV/vis, or luminescent spectroscopy. In addition, it is possible to study the reactivity of the intermediates in various unimolecular and bimolecular processes. For the silica powders with large specific surface (ca. 100 m^2/g), the concentration of the surface defects (or products of their modification) may be as high as $10^{18}-10^{19}$ g^{-1}.

Experimental Section

Silica powders with high dispersity (aerosil) were used. The specific surface of the activated samples was 100−150 m^2/g as measured by adsorption of N_2 or Ar at 77 K. The techniques of sample preparation and surface activation were described previously.[14,15]

The structure and the concentration of the surface defects trapped at the silica surface prepared using various activation techniques are given in Table 1.

Commercial gases (ethylene, 1,3-butadiene, and cyclopropane) were used as received (the content of impurities in these gases did not exceed 2%). Carbon monooxide and formaldehyde were prepared by standard procedures (i.e., by interaction of concentrated formic and sulfuric acids, and by thermal decomposition of paraform, respectively).

Photolysis of the samples was carried out with a high-pressure mercury lamp. Glass filters were used to separate the spectral region of $\lambda \geq 370$ nm. ESR spectra were measured with the X-band spectrometers with high-frequency modulation of 100 kHz in the temperature range 77−500 K.

Isotropic hyperfine splitting constants were determined from anisotropic ESR spectra assuming axial symmetry of corresponding tensors: $a_{iso} = (2a_{\perp} + a_{||})/3$. In some cases, the parameters of the spin Hamiltonian were corrected from the comparison of the experimental and calculated ESR spectra. The program used made it possible to calculate the intensities of allowed transitions in the frame of the first-order perturbation theory for isotropic or axially symmetrical g and a tensors. Lorentzian line shape was assumed in the simulation of the ESR spectra.

Ab initio SCF MO LCAO calculations were carried out using Gaussian code.[17] The unrestricted version of the Hartree−Fock calculational scheme (UHF, UMP2) was used. Gradient technique with the 6-31G* basis set completed with 6d polarization functions for heavy atoms was used in optimization of the geometry of molecules and radicals. Partial account of the effects of electron correlation was performed using the Moeller−Plesset theory of second-order perturbations.

Isotropic hyperfine coupling constants were determined from the values of Fermi contact components $|\psi_n(0)|^2$:

$$a_{iso} = (8\pi/3)g_e\beta_e g_n\beta_n|\psi_n(0)|^2 = a_0(n)|\psi_n(0)|^2$$

where $|\psi_n(0)|^2$ is the electron spin density at the nucleus n. If the values of $|\psi_n(0)|^2$ are expressed in atomic units, one should use $a_0(^1H) = 159.5$ mT and $a_0(^{29}Si) = -31.7$ mT.

Results and Discussion

Table 2 summarizes the chemical reactions used for preparation of the various types of grafted allyl radicals; the reaction conditions are also given.

The differences in the structure of allyl radicals have a pronounced effect on the shape of the corresponding ESR spectra (Figure 1), which allowed us to make unambiguous identification of the spectra. The parameters of the ESR spectra of allyl radicals **I**−**VII** are listed in Table 3.

Photolysis of the samples containing substituted allyl radicals **I**−**IV** results in the multifold decrease in the intensity of the ESR signals of allyl radicals and the appearance of a new spectrum. The total concentration of radicals in the system under study remains unchanged. Figure 2a shows the ESR spectrum of the product of phototransformation. The ESR signals of similar shape were also recorded upon photolysis of allyl radicals **I**−**III**. The resulting radicals are stable in the temperature range 77 to 230−260 K (the upper limit of thermal stability is different for the different radicals). Measurement of the ESR spectra of these radicals at the temperatures near the upper limit of their thermal stability results in the remarkable increase of a spectral resolution (Figure 2). The changes of the shape of the ESR signals with temperature are reversible.

We have assigned the observed ESR signals to the β-substituted cyclopropyl radicals resulting from photochemical cyclization of the allyl-type radicals in the region of long-wave absorbtion band (Figure 3):

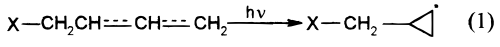

(1)

The hyperfine coupling constants for β-substituted cyclopropyl radicals resulting from photolysis of radicals **I**, **II**, and **IV**, aligned with the spectroscopic characteristics of the cyclopropyl radical, are given in Table 4.

Two additional lines of low intensity were detected in the ESR spectrum of radical **VIII** (Figure 4). These extra lines are due to the coupling of an unpaired electron with the ^{29}Si isotope nucleus in β-position (natural abundance of ^{29}Si is 4.7%). The value of the corresponding hyperfine coupling constant decreases with increase of the temperature (Table 4). Another feature of the ESR spectrum of radical **VIII** is concerned with the doublet structure of the outermost components (Figure 4). The corresponding coupling constant is ca. 0.1 mT. In our view, this doublet is due to hyperfine coupling of unpaired electrons with hydroxyl protons. Note that the significant difference of the hyperfine coupling constants for the various β-protons is characteristic of radical **IX**. The ESR spectrum of this radical

TABLE 2: Chemical Reactions Used for Preparing Various Types of Grafted Allyl Radicals

N	Radical	Reactons
I	≡Si(OH)CH···CH···CH$_2$	≡SiO$^\bullet$ + △ $\xrightarrow{200\ K}$ ≡SiOH + △ =Si=O + △$^\bullet$ $\xrightarrow{200\ K}$ =SiOH—△$^\bullet$ =SiOH—△$^\bullet$ $\xrightarrow{200\ K}$ =Si(OH)CH···CH···CH$_2$
II	=Si(OH)OCH···CH···CH$_2$	=Si(O)$_2$ + △ $\xrightarrow{200\ K}$ =Si(O$^\bullet$)OH + △$^\bullet$ =Si(O$^\bullet$)OH + △ $\xrightarrow{200\ K}$ =Si(OH)$_2$ + △$^\bullet$ =Si(O)$_2$ + △$^\bullet$ $\xrightarrow{200\ K}$ =Si(O—△$^\bullet$)OH =Si(O—△$^\bullet$)OH $\xrightarrow{300\ K}$ =Si(OH)OCH···CH···CH$_2$
III	≡SiCH$_2$CH···CH···CH$_2$	≡Si$^\bullet$ + CH$_2$=CHCH=CH$_2$ $\xrightarrow{300\ K}$ ≡SiCH$_2$CH···CH···CH$_2$
IV	≡SiOCH$_2$CH···CH···CH$_2$	≡SiO$^\bullet$ + CH$_2$=CHCH=CH$_2$ $\xrightarrow{300\ K}$ ≡SiOCH$_2$CH···CH···CH$_2$
V	≡SiO(CH$_2$)$_2$CH···CH···CH$_2$	≡Si$^\bullet$ + CH$_2$=O $\xrightarrow{300\ K}$ ≡SiOCH$_2^\bullet$ ≡SiOCH$_2^\bullet$ + CH$_2$=CHCH=CH$_2$ $\xrightarrow{300\ K}$ ≡SiO(CH$_2$)$_2$CH···CH···CH$_2$
VI	≡Si(CH$_2$)$_3$CH···CH···CH$_2$	≡Si$^\bullet$ + CH$_2$CH$_2$ $\xrightarrow{195\ K}$ ≡SiCH$_2$CH$_2^\bullet$ ≡SiCH$_2$CH$_2^\bullet$ + CH$_2$=CHCH=CH$_2$ $\xrightarrow{300\ K}$ ≡Si(CH$_2$)$_3$CH···CH···CH$_2$
VII	≡SiO(CH$_2$)$_3$CH···CH···CH$_2$	≡SiO$^\bullet$ + CH$_2$CH$_2$ $\xrightarrow{195\ K}$ ≡SiOCH$_2$CH$_2^\bullet$ ≡SiOCH$_2$CH$_2^\bullet$ + CH$_2$=CHCH=CH$_2$ $\xrightarrow{300\ K}$ ≡SiO(CH$_2$)$_3$CH···CH···CH$_2$

also exhibits an additional splitting of the components of hyperfine structure. Similar to the case of radical **VIII**, we attribute this splitting to the coupling of an unpaired electron with the proton of neighboring hydroxyl groups.

To assign the experimental hyperfine splitting constants to the specific β-protons in substituted cyclopropyl radicals, we have carried out the quantum-chemical calculations of the corresponding characteristics for a series of simple β-substituted cyclopropyl radicals of the structure X-c-Pr$^\bullet$, where X = H, CH, SiH, OH, or F. The equilibrium geometric characteristics of these radicals (with the exception of HO-c-Pr$^\bullet$) were calculated previously at various theoretical levels (X = H,[2,19] CH_3 and SiH_3,[20] F[21,22]). The $\langle S^2 \rangle$ values for the optimized radical structures deviate only slightly from 0.75 (the latter value corresponds to the doublet state of the system). This result demonstrates that the calculations using the unrestricted version of the Hartree−Fock scheme describe reasonably well the free-radical (doublet) state in the systems under consideration.

Cyclopropyl-type radicals are known to be σ-radicals.[2,23] This implies that the unpaired electron occupies the hybrid orbital of the three-coordinated carbon atom, and the β-hydrogen atom bound to this carbon is out of the ring plane. As a result, two conformers may exist. Interconversion of the conformers occurs by inversion of the β-hydrogen. According to refs 20 and 22, the difference in the electronic energies of the conformers does not exceed 1 kcal/mol. $\Delta H_0(0)$ values (enthalpies at 0 K) determining the thermodynamic stability of the conformers depend also on the zero potential energy (ZPE) of the system. The ZPE values are close for cis- and trans-conformers, so the differences in the $\Delta H_0(0)$ values of the conformers do not result from the variations in ZPE. The $\Delta H_0(0)$ values for the allyl radicals with various substituents increase in the following order: $CH_3 < SiH_3 < F < OH$. The trans-conformation was found to be more stable for silyl-substituted radical,[20] whereas the cis-conformation was favorable in the cases of the radicals substituted with F[21,22] or OH (this work).

Satisfactory results were obtained in the calculations of the hyperfine coupling constants for cyclopropyl radical;[19] these calculations used extended basis sets and took into account the effects of electron correlation. The values of isotropic hyperfine coupling constants for α- and β-protons in the cyclopropyl-type radicals calculated from the Fermi contact components at the UHF/6-31G* level are listed in Table 5. In these radicals the β-protons of methylene groups are characterized by essentially different coupling constants. The calculated values of the hyperfine coupling constants for cyclopropyl radical are $a_H(\alpha) = -1.96$ (−0.57) mT, $a_H(\beta_1) = 2.47$ (2.33) mT, and $a_H(\beta_2) = 1.63$ (1.38) mT (the results from ref 19 are given in parentheses). According to refs 18 and 24, β-protons in cyclopropyl radical exhibit similar hyperfine coupling constants because of the high frequency of the inversion of the α-proton ($n \gg 10^8$ s^{-1}). In this case, $a_H(\beta_1) = a_H(\beta_2) = 1/2(a_H(\beta_1) + a_H(\beta_2)) = 2.05$ mT. As a result, the ratios of calculated (UHF/6-31G*) to experimental hyperfine coupling constants for α- and β-protons are 0.33 and 1.14, respectively. The calculated hyperfine coupling constants with α- and β-protons in other radicals were corrected using these scaling factors (the corresponding values are given in Table 5 in parentheses). The

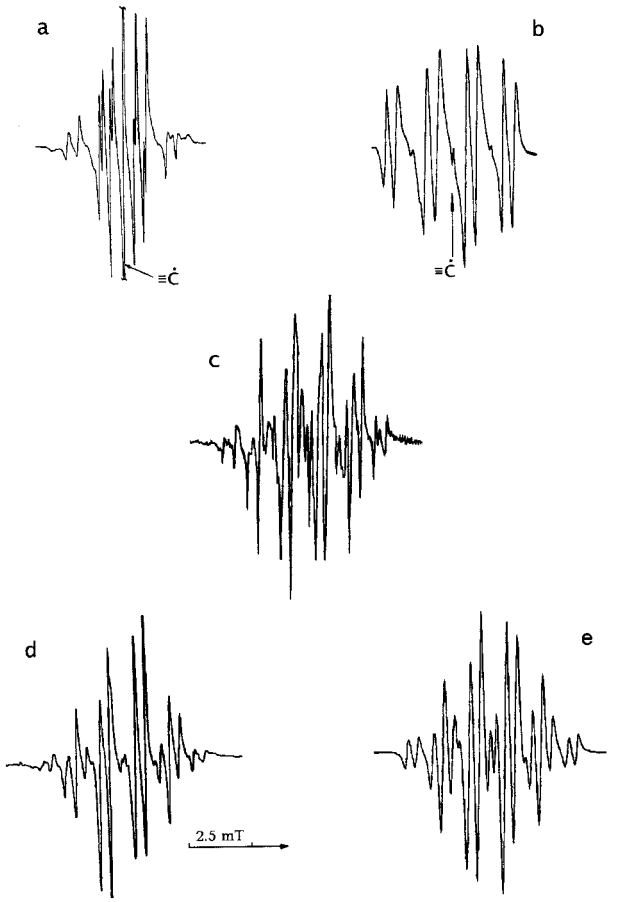

Figure 1. ESR spectra of radicals on activated silica surface at different temperatures: **I**, 470 K (a); **II**, 540 K (b); **III**, 293 K (c); **IV**, 293 K (d); calculated ESR spectra of radical **IV**, 293 K (e).

TABLE 3: Hyperfine Coupling Constants (mT) in Substituted Allyl Radicals Grafted onto Silica Surface[a]

radical	hyperfine coupling constants (mT)
I	3H, $a = 1.40$; 1H, $a = 0.50$; 1H, $a = 0.20$
II	3H, $a = 1.46$; 1H, $a = 0.34$
III	3H, $a = 1.41$; 2H, $a = 1.07$; 1H, $a = 0.42$
IV	3H, $a = 1.40$; 2H, $a = 1.00$; 1H, $a = 0.38$
V	2H, $a = 1.37$; 2H, $a = 1.19$; 1H, $a = 0.42$; 1H, $a = 0.38$
VI	3H, $a = 1.40$; 2H, $a = 1.25$; 1H, $a = 0.38$
VII	3H, $a = 1.40$; 2H, $a = 1.20$; 1H, $a = 0.40$

[a] The hyperfine coupling constants for the radical **I** were measured at 77 K, for the radicals **II**−**VII** at 293 K.

corrected parameters were used for the interpretation of the experimental data.

Among the cyclopropyl-type radicals the oxygen-substituted species **IX** exhibits an essential difference in the hyperfine splitting constants from other radicals. The comparison of the observed hyperfine coupling constants with the calculated values for F- and OH-substituted radicals shows that the experimental values are close to the calculated constants for the more stable cis-isomer. For this reason, we attribute the constant of 1.85 mT to the CH β-proton and two other constants to CH_2 protons.

In the case of silyl-substituted cyclopropyl radical **VIII**, the constant of 2.86 ± 0.05 mT may be due to a β-proton at the substituted carbon atom, whereas two other constants of roughly the same magnitude may be ascribed to CH_2 protons. The close values of the constants associated with two protons of the methylene groups indicate that both conformations of the radical are characterized by nearly equal energies ($\Delta E < 0.2$ kcal/mol). The hyperfine coupling constant with the silicon atom in the

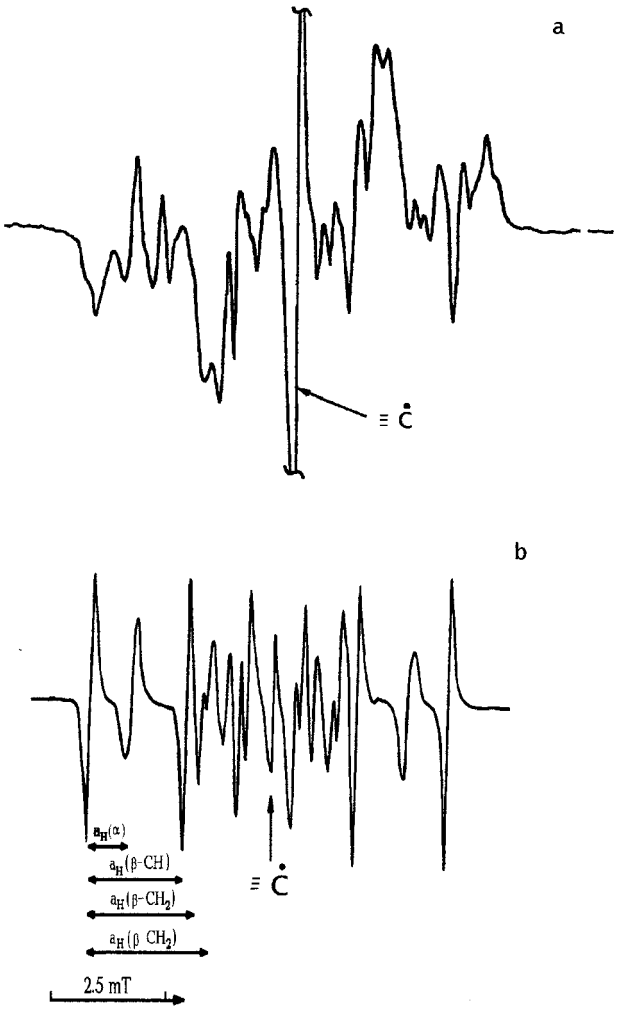

Figure 2. ESR spectra of radical **X** at 77 (a) and 260 K (b).

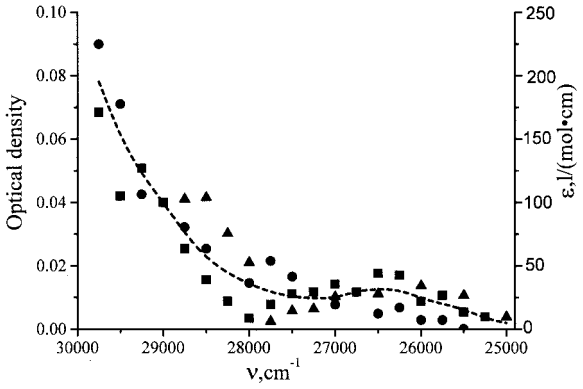

Figure 3. UV-absorption spectra of allyl-type radical in 3-ethylpentene-2 at 77 K.[4]

radical under consideration shows a negative temperature coefficient. This observation is in agreement with the results of quantum-chemical calculations, which predict that the trans-conformation with larger coupling constant is more stable.

Warming of the photoirradiated samples up to 240−300 K results in irreversible disappearance of the lines of the product of phototransformation and simultaneous recovering of the initial intensity of the ESR signal from allyl radicals **I**−**IV** (Figure 6). This result is due to reverse reaction 1 occurring upon warming of the sample. The thermal transformations of this kind are typical for cyclopropyl-type radicals.[23] Kinetic curves of thermal transformation of cyclopropyl radicals to allyl radicals

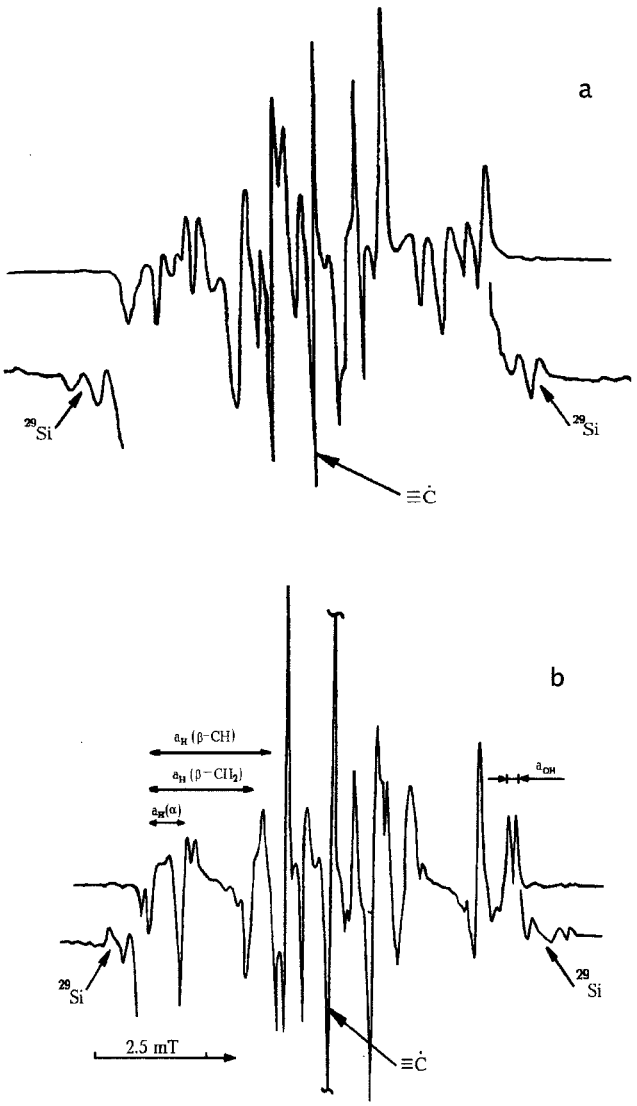

Figure 4. ESR spectra of radical **VIII** at 77 (a) and 243 K (b).

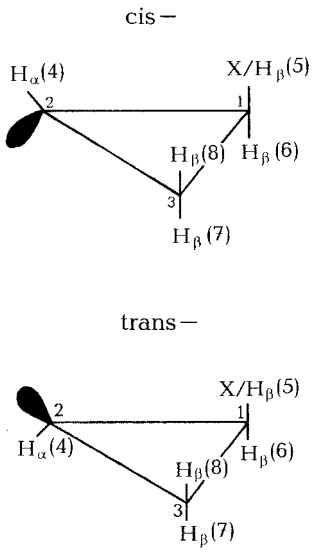

Figure 5. Numbering of atoms in β-substituted cyclopropyl radicals.

show satisfactory linearity if plotted in the first-order coordinates. The rate constants of the thermal reactions of radicals **VIII**−**X** and the estimated activation energies are given in Table 6. The results presented in Table 6 show that the presence of an electron-withdrawing substituent results in the decrease in the thermal stability of the cyclopropyl radical. The destabilizing effect of electron-withdrawing groups on the cyclopropyl ring was reported previously.[22,27] This conclusion is supported by the results of the quantum-chemical calculations. We have carried out a comparative study of transitional states (TS) and activation energies for ring opening in cyclopropyl and β-fluorocyclopropyl radicals. According to the results of semiempirical (MINDO/3)[29] and ab initio (CASSCF/3-21G)[20] calculations, the transitional state for the transformation of cyclopropyl to allyl radical is unsymmetric. The rotation of one of the methylene groups is accompanied by shortening of the corresponding $C_\alpha-C_\beta$ bond, whereas the length of the other $C_\alpha-C_\beta$ bond remains practically unchanged. Respectively, the change in the orientation of the latter methylene group relative to the carbon skeleton plane is negligible.

The calculations at CASSCF/3-21G*[20] and UHF/6-31G* (this work) levels result in close geometries of the transitional state. However, taking into account the effects of electron correlation (UMP2/6-31G*) results in significant increase in the difference of the C−C bond lengths in the transitional state. In this case, the angle of rotation of the CH_2 group (in the C_3H_5 radical) or the CHF group (in the C_3H_4F radical) relative to the carbon skeleton plane increases, and the length of the corresponding C−C bond becomes close to the length of the C=C double bond in alkenes. The $\langle S^2\rangle$ values for allyl and transitional structures are considerably higher than the value of 0.75 corresponding to doublet state of the system. This result bears evidence for the contribution of the states with higher multiplicity into the wave function, which leads to overestimation of the energies of the calculated structures. The PUMP2/6-31G*//UMP2/6-31G* calculations using spin-projected wave functions result in a better agreement between the experimental and the calculated values of reaction heats and activation energies for the interconversion between allyl and cyclopropyl radicals. According to the results of calculations, the presence of fluorine atom in the β-position of cyclopropyl radical results in the decrease of the activation energy of ring opening by 6.5 kcal/mol. In addition, the heat of the reaction increases by ca. 3 kcal/mol for the fluorine-substituted radical (as compared to cyclopropyl radical).

Therefore, an electron-withdrawing substituent has a larger effect on kinetic stability of the cyclopropyl radical (decreasing of the activation energy of ring opening) than on thermodynamic characteristics (reaction heat).

The experimental data obtained in this work show that in the case of radicals **I** and **II** the total concentration of paramagnetic species remains constant upon phototransformation of allyl radical to cyclopropyl radical and back by thermal reaction; that is the reaction 1 is fully reversible. This result implies that photocyclization is the predominating pathway of the photochemical transformations of these radicals.

As mentioned above, we failed to detect the formation of the products of intramolecular hydrogen transfer as a result of thermal isomerization of cyclopropyl-type radicals

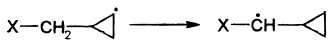

for radicals **III** and **IV**. The reason for the absence of this process is that the 1,3-migration of hydrogen atoms in hydrocarbon radicals is characterized by the activation energy of ca. 40 kcal/mol.[29] This value is higher than the value of activation energy required for the isomerization of cyclopropyl radical to allyl radical.

TABLE 4: Hyperfine Coupling Constants (mT) in Substituted Cyclopropyl Radicals Grafted onto Silica Surface

Radical	T, K	$a_H(\alpha)$	$a_H(\beta\text{-}CH_2)$	$a_H(\beta\text{-}CH)$	$a_H(OH)$	$a(^{29}Si)$
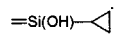 VIII	243 77	0.69±0.05	2.19±0.05 2.19±0.05	2.86±0.05	≈ 0.10	2.50±0.10 3.05±0.15
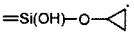 IX	203 77	0.84±0.05	2.46±0.03 3.69±0.04	1.87±0.02		
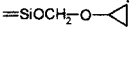 X	260 77	0.86±0.03	2.45±0.02 2.59±0.02	2.11±0.02		
 [18]	143	0.65	2.34			

TABLE 5: Calculated Hyperfine Coupling Constants (mT) with α- and *β*-Protons in Substituted Cyclopropyl Radicals

Y[a]	CH_3 (trans)	CH_3 (cis)	SiH_3 (trans)	SiH_3 (cis)	F (trans)	F (cis)	OH (trans)	OH (cis)
α-H	-1.96 (-0.65)	-1.98 (-0.65)	-1.77 (-0.58)	-1.80 (-0.60)	-2.50 (-0.83)	-2.44 (-0.81)	-2.31 (-0.81)	-2.18 (-0.72)
H(7)	1.64 (1.87)	2.49 (2.84)	1.45 (1.65)	2.28 (2.60)	2.23 (2.55)	2.93 (3.35)	2.01 (2.29)	2.74 (3.13)
H(8)	2.52 (2.87)	1.56 (1.78)	2.18 (2.49)	1.47 (1.67)	3.35 (3.82)	2.07 (2.36)	3.05 (3.47)	1.83 (2.09)
H(6)	1.53 (1.75)	2.63 (3.00)	2.10 (2.40)	2.85 (3.25)	0.83 (0.95)	1.63 (1.85)	0.92 (1.05)	1.90 (2.16)
β-Si			1.75	1.00				

[a] The numbering of atoms in substituted cyclopropyl radicals illustrated in Figure 5.

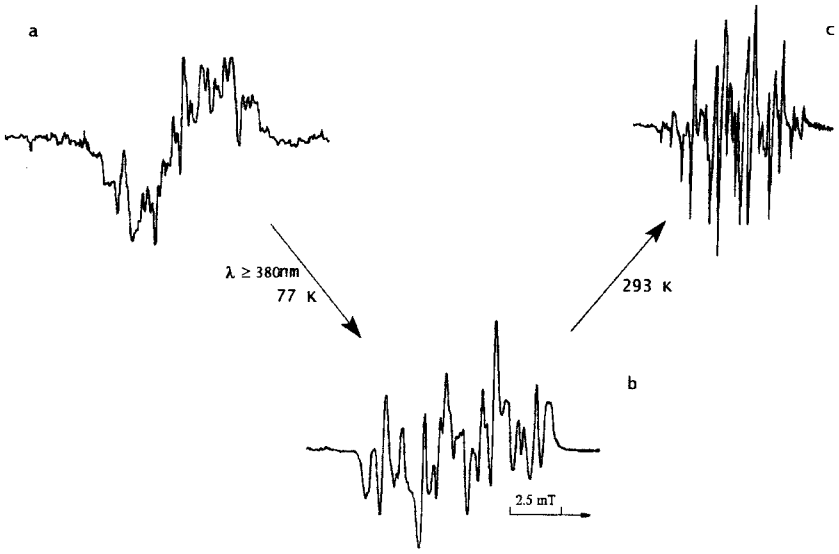

Figure 6. ESR spectra before (a) and after (b) irradiation ($\lambda \geq 380$ nm) of radical **III** at 77 K; (c) after warming of sample (b) to 293 K.

In the case of radicals **V**−**VII**, one should expect increase of the contribution of the process resulting in the formation of the product of intramolecular hydrogen transfer. In particular, photolysis of radical **V** results in the formation of a cyclopropyl-type radical, similarly to the case of radicals **I**−**IV**. However, the thermal transformations in this system occur at lower temperatures (from 180 K) and are accompanied by the formation of alkyl radicals of the structure ≡Si−O−ĊH−CH_2∼. The ESR spectrum of the latter radicals (Figure 7) is due to coupling of an unpaired electron with one α-proton (hyperfine coupling constant of 1.95 mT) and two magnetically equivalent *β*-protons (coupling constant of 2.14 mT). Thus, the thermal transformation of radical V occurs via intramolecular hydrogen atom transfer (1,4-migration). If the reaction is carried out at

TABLE 6: Rate Constants and Activation Energies of Thermal Transformations of *β*-Substituted Cyclopropyl Radicals into Allyl Radicals

radical	*T*, K	*k*, s^{-1}	*E*, kcal/mol[a]
VIII	260	$(1.4 \pm 0.1) \times 10^{-3}$	≈19
IX	214	$(9.8 \pm 0.5) \times 10^{-4}$	≈16
X	275	$(3.5 \pm 0.2) \times 10^{-4}$	≈20−21
	291	$(3.8 \pm 0.2) \times 10^{-3}$	

[a] According to the data,[19,20] the value of k_0 is equal to 10^{13} s^{-1}.

TABLE 7: Energetic Characteristics of the Transformation of Cyclopropyl and β-Substituted Fluorocyclopropyl into Allyl Radicals (kcal/mol)

	$C_3H_5^•$	TS	c-Pr$^•$	$C_3H_4F^•$	TS	F-c-Pr$^•$
$-E$(UMP2)	116.81022	116.71723	116.77791	215.82746	215.74502	215.79083
$\langle S^2\rangle^a$	0.96(0.76)	1.13(0.76)	0.76(0.75)	0.95(0.76)	1.02(0.76)	0.76(0.75)
ΔE	−20.3	38.1	0.0	−23.0	28.7	0.0
$-E$(PUMP2)	116.82485	116.73513	116.77951	215.84201	215.75978	215.79245
ΔE	−28.5	27.9	0.0	−31.1	20.5	0.0
ZPE^b	43.7	41.9	44.9	39.1	38.3	40.5
$\Delta H_0(0)$	−29.7	24.9	0.0	−32.5	18.3	0.0
$\Delta H_0(0)^c$	−35.5	21.9	0.0			

[a] The values in parentheses were obtained by using spin-projected wave function. [b] The values were calculated in harmonic approximation at UHF/6-31G*. [c] The data of ref 21.

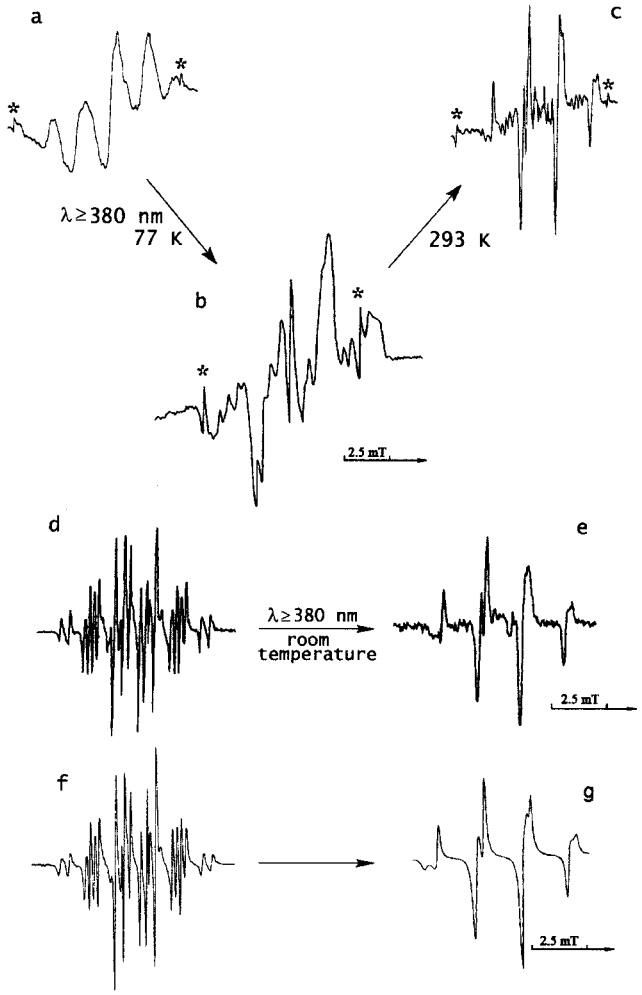

Figure 7. ESR spectra before (a) and after (b) irradiation ($\lambda \geq 380$ nm) of radical **V** at 77 K; (c) after warming of sample (b) to 293 K; before (d) and after (e) irradiation ($\lambda \geq 380$ nm) of radical **V** at 293 K; calculated ESR spectra of radical **V** (f) and radical product of their photoconversion (g) at 293 K.

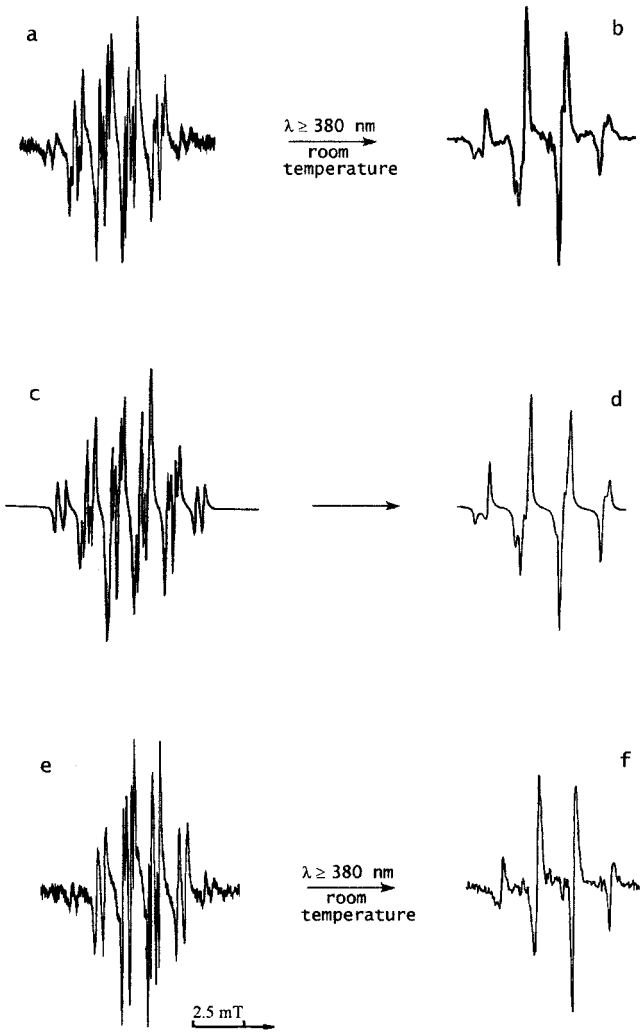

Figure 8. ESR spectra before (a, e) and after (b, f) irradiation ($\lambda \geq 380$ nm) of radical **VI** (a, b) and **VII** (e, f) at 293 K. Calculated ESR spectra of radical **VI** (c) and the radical product of their photoconversion (d) at 293 K.

room temperature (and not at 77 K), radical ≡Si−O−$\dot{C}$H−CH_2∼ is the only observable product.

Increase of the length of the aliphatic chain by one more methylene group (radicals **VI** and **VII**) results in the formation of radicals of the structure ≡Si−O−$\dot{C}$H−CH_2∼ (or ≡Si−$\dot{C}$H−CH_2∼) immediately after photolysis at 77 K (in addition to small amounts of cyclopropyl-type radicals). This means that the reaction of intramolecular hydrogen transfer occurs even at 77 K in this case. It is natural that radicals ≡Si−O−$\dot{C}$H−CH_2∼ or ≡Si−CH−$\dot{C}H_2$∼ are the main products of the photolysis of radicals **VI** or **VII**, respectively, at 300 K (Figure 8).

In our view, the presence of substituents in the radicals under study (radicals **III**−**VII**) might result in the appearance of the photolytic pathways associated with abstraction or intramolecular migration of hydrogen atoms, e.g.,

$$\equiv SiOCH_2CH\cdots CH\cdots CH_2 \xrightarrow{h\nu} \equiv SiOCH{=}CH{-}CH{=}CH_2 + H \quad \text{or}$$

$$\equiv SiOCH_2CH\cdots CH\cdots CH_2 \xrightarrow{h\nu} \equiv SiOCH\cdots CH\cdots CHCH_3$$

However, even if the processes of this kind occur upon photolysis, their efficiency is less than that of photocyclization, at least by an order of magnitude.

Thus, the experimental data obtained in this work indicate that β-substituted cyclopropyl radicals are the primary products of the photochemical transformation of allyl-type radicals with light of $\lambda \geq 370$ nm. Subsequent thermal reactions of cyclopropyl-type radicals are controlled by their structure and may result in the formation of various final products.

Conclusions

The technique used in this study can be applied for the investigations of various processes. In addition to the reactions of isomerization of cyclopropyl-type radicals with ring opening and hydrogen atom abstraction from alkyl substituents, it is also possible to examine the bimolecular reactions.

In particular, we observed that the phototransformations of allyl radicals **III**−**V** in all cases were accompanied by the decrease in the total amount of radicals. A maximum effect of this kind was observed for radical **VII** (40−50% at virtually complete conversion of the radical). Since allyl-type radicals show low reactivity in the reactions of addition or substitution at room temperature, we ascribe the observed decay to the formation of the reactive cyclopropyl-type radicals upon photolysis. The most probable process resulting in the radical decay at the surface is concerned with step-by-step radical site migration due to the interaction of small free radicals resulting, for example, from the reaction of the cyclopropyl-type radicals with residual molecules of organic compounds present in the system. This conclusion is based on the assumption of high (and comparable) mobility of molecules and radicals adsorbed on the aerosil surface. This assumption is supported by the data on the values of diffusion coefficients measured for the molecules of methyl methacrylate and vinyl acetate at aerosil surfaces ($>10^{-6}$ cm^2/s[30]).

The reaction of cyclopropyl-type radicals with formaldehyde molecules should result in the formation of HCO radicals, which may induce the decay of paramagnetic species at the surface. On the other hand, the reactions of addition of, for example, 1,3-butadiene followed by photocyclization of the resulting allyl-type radicals, i.e.,

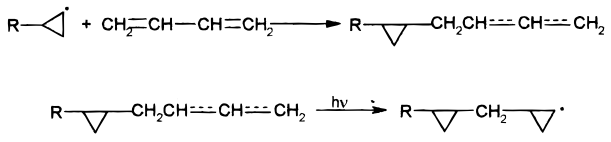

may induce a specific kind of photopolymerization of 1,3-butadiene. The work to verify this hypothesis is in progress now.

Acknowledgment. This work was supported by the Russian Foundation for Basic Research (Grants 95-03-08119 and 96-03-32440).

References and Notes

(1) Carsky, P. *J.Phys. Chem.* **1970**, *74*, 1249−1254.
(2) Ha Tae-Kyu; Baumann, H.; Oth, J. *J.Chem. Phys.* **1986**, *85*, 1438−1442.
(3) Roginskii, V. A.; Pschezheckii, S. Ya. *Khim. Vys. Energ.* **1969**, *3*, 140−146 (in Russian).
(4) Pergushov, V. I. *Vestn. Mosk. Univ., Khim.* **1993**, *34*, 473−476 (in Russian).
(5) Simada, S.; Kashiwabara, H.; Sohma, J. *J. Polym. Sci., A-2*. **1970**, *8*, 1291−1302.
(6) Tsuji, K. *J. Polym. Sci., Polym. Chem. Ed.* **1973**, *11*, 467−484.
(7) Roginskii, V. A.; Pschezheckii, S. Ya. *Khim. Vys. Energ.* **1970**, *4*, 240−245 (in Russian).
(8) Roginskii, V. A. *Khim. Vys. Energ.* **1969**, *3*, 473−475 (in Russian).
(9) Smith, D. R.; Okernka, F.; Pieroni, J. J. *Can. J. Chem.* **1967**, *45*, 833−837.
(10) Holtzhauer, K.; Cometta-Morini, C.; Oth, J. E. M. *J. Phys. Org. Chem.* **1990**, *3*, 219−229.
(11) Radzig, V. A. *Kinet. Katal*. **1983**, *24*, 173−180 (in Russian).
(12) Radzig, V. A. *Khim. Fiz.* **1995**, *14*, 125−154 (in Russian).
(13) Radzig, V. A.; Bystrikov, A. V. *Kinet. Katal*. **1978**, *19*, 713−718 (in Russian).
(14) Radzig, V. A. *Khim. Fiz.* **1991**, *10*, 1262−1279 (in Russian).
(15) Osokina, N. Yu.; Razskazovskii, Yu. V.; Pergushov, V. I.; Mel'nikov, M. Ya. *Z. Fiz. Khim.* **1995**, *69*, 1858−1862 (in Russian).
(16) Bobyshev, A. A.; Radzig, V. A. *Kinet. Katal*. **1990**, *31*, 925−930 (in Russian).
(17) Hehre, W. J.; Radom, L.; Schleyer, P. v. R.; Pople, J. A. *Ab initio Molecular Orbital Theory*; Wiley Interscience, Publ: New York, 1986.
(18) Fessenden, R. W.; Schuler, R. H. *J. Chem. Phys.* **1963**, *39*, 2147−2195.
(19) Barone, V.; Minichino, C.; Faucher, H. *Chem. Phys. Lett.* **1993**, *205*, 324−330.
(20) Olivella, S.; Sole, A.; Bofill, J. M. *J. Am. Chem. Soc.* **1990**, *112*, 2160−2167.
(21) Ibrahim, M. R.; Jorgensen, W. L. *J. Am. Chem. Soc.* **1989**, *111*, 819−824.
(22) Clark, T.; Kos, A. J.; Schleyer, P. v. R.; Coffino, W. P., de Wolf, W. H.; Bickelhaupt, F. *J. Chem. Soc., Chem. Commun.* **1983**, 685−687.
(23) Walborsky, H. M. *Tetrahedron.* **1981**, *37*, 1625−1651.
(24) Ohmae, T.; Ohnishi, S.; Kumata, K. *Bull. Chem. Soc. Jpn.* **1967**, *40*, 226−228.
(25) Greig, G.; Thynne, J. C. J. *Trans. Faraday Soc.* **1967**, *63*, 1369−1374.
(26) Walsh, R. *Int. J. Chem. Kinet.* **1970**, *2*, 71−74.
(27) Getty, S. J.; Hrovad, D. A.; Borden, W. T. *J. Am. Chem. Soc.* **1994**, *116*, 1521−1527.
(28) Dewar, M. J. S.; Kirchner, S. *J. Am. Chem. Soc.* **1971**, *93*, 4290−4292.
(29) Frey, H. M.; Walsh, R. *Chem. Rev.* **1969**, *69*, 103−124.
(30) Bruk, M. A., Pavlov, S. A. *Polimerizaciya na poverkhnosti tverdykh tel*; Khimiya: Moscow, 1990 (in Russian).